RSC Advances

PAPER

View Article Online
View Journal | View Issue

Cite this: *RSC Adv.*, 2018, **8**, 12684

Preparation of a novel polyacrylic acid and chitosan interpenetrating network hydrogel for removal of U(VI) from aqueous solutions

Jiarui He, Fuliang Sun, Fuhao Han, Junjie Gu, Minrui Ou, Wenkai Xu and Xiaoping Xu *

A clean and simple method has been developed for preparation of interpenetrating polymer networks using polyacrylic acid (PAA) and chitosan (CS) for extraction of uranium from polluted water. The peak of Fourier transform infrared spectroscopy (FTIR) occurred at 928 cm^{-1} indicating combination of uranium and PAA/CS. The energy dispersive X-ray (EDX) and the scanning electron microscope (SEM) studies illustrated the formation of a crosslinking structure and excellent binding ability of uranium on PAA/CS. The maximum adsorption capacity was 289.6 mg g^{-1} calculated using the equation of the Langmuir model. The adsorption capacity reached a plateau at pH 4 and the sorption process fits the pseudo-second-order model well. The PAA/CS composite has stability of reuse, with the adsorbent capacity decreasing slowly with increasing usage frequency. The experimental results confirm that the PAA/CS hydrogel could be a novel alternative for highly efficient removal of uranium from wastewater.

Received 6th December 2017
Accepted 9th March 2018

DOI: 10.1039/c7ra13065a

rsc.li/rsc-advances

1. Introduction

Conventional energy sources from the degradation of coal and petroleum cause serious environmental and human health problems. The high speed development of nuclear energy as an alternative means that various radionuclides are being released into the environment from the legacy of mining, nuclear reactors, and activities of nuclear weapons.[1] The uranium ion is one of the most common contaminating ions, with high radiation and chemical toxicity. Therefore, focus in recent years has been on how to reduce the uranium ion content in drinking water. Although various methods are available to reduce uptake of radioactive elements in various fields, efficient techniques are still required.

There are many physical and chemical methods for removal of uranium from wastewater including instance ion-exchange processes,[2] solvent extraction,[3] surface complexation, and adsorption.[4–6] Adsorption has been used by many plants and enterprises because of its excellent performance, easy operation, low consumption, high efficiency, and environmental friendliness.[7–10] A variety of materials have been extensively studied for adsorption. Traditional materials for extraction of uranium ions from aqueous solution, such as carbon,[11,12] zeolite,[13] clay,[14] composites,[15] natural polymers,[16] and synthetic polymers,[17] have abundant pores or functional groups. Among them, the binding capacity of chitosan is higher than that of commercial adsorbents, it is cheap and rich in nature, so it is of great interest to researchers for remediation of metal ions.[18,19] However, the raw material of particle chitosan is usually difficult to recycle after adsorption reaction. Hydrogel, one of the most widely used polymers, consists of a three-dimensional network of hydrophilic polymers which allows diffusion of solutes into the interior network, and can be prepared using a covalent or a non-covalent approach with different functional groups such as carboxylic acid, hydroxyl and amine groups.[18,19] PAA hydrogel has a specific adsorption capacity based on the mutual attraction between carboxyl and metal cations, and its synthetic steps are relatively timely, convenient, and flexible.[20] Compared with chitosan, PAA has a stable and water insoluble structure. Furthermore, the bulk gel prepared from acrylic monomer holds recycle performance, hence research into CS/PAA composites is desirable.

In this work, a PAA-chitosan interpenetrating network is fabricated for sorption of uranium in potable water. The pH, contact time, and initial concentration were assessed by batch adsorption tests. The adsorption performance and mechanism were investigated by kinetic and isotherm models. PAA/CS composites were reused five times to predict properties of sustainable utilization. The experimental results indicate that the PAA/CS hydrogel has much potential in disposal of sewage.

2. Experimental

2.1. Materials

Acrylic acid (AA) and methylene-bis-acrylamide (MBA) were purchased from Sinopharm Chemical Reagent Co., Ltd. Chitosan (CS) and sodium hydrogen sulfite (SHS) were provided by

College of Chemistry, Fuzhou University, Fuzhou, 350108, China. E-mail: xu@fzu.edu.cn

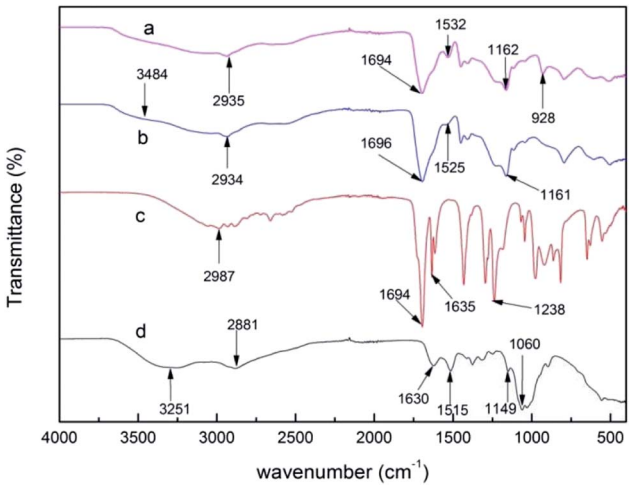

Fig. 1 Fourier transform-infrared (FT-IR) spectra of (a) U-PAA/CS, (b) PAA/CS, (c) AA and (d) CS.

Xilong Chemical Co., Ltd. Ammonium persulfate (APS) was supplied by Shanghai SANGON Biological Engineering Co., Ltd, China. A uranium stock solution (1000 mg L^{-1}) was prepared by adding $UO_2(NO_3)_2 \cdot 6H_2O$ to deionized water. All chemicals used in this study were of analytical grade.

2.2. Preparation of PAA/CS

The chitosan (2 g) was dissolved in a beaker of acetic acid solution with a mass fraction of 20% by stirring for about 20 min at room temperature, and about 0.20 g APS and 0.20 g SHS was added to the solution with slow stirring. Then the acrylic monomer (14 mL) and 0.48 g MBA were put into a beaker, with ultrasound for 10 minutes. One of the solutions was poured into the other after both solutes were well-distributed. After the hydrogel formed, the product was washed with deionized water several times. Finally, the obtained hydrogel was dried in a vacuum freeze-drying machine for 12 h and stored in a vacuum drying oven at 55 °C.

2.3. Instrumentation

FTIR (Fourier transform infrared spectroscopy) of the samples was analyzed using a FTIR spectrophotometer in the range of 4000–400 cm^{-1}.

SEM (scanning electron microscope) analysis of PAA/CS and PAA/CS after adsorption were recorded using Nova Nano 230 apparatus.

EDX (energy dispersive X-ray) measurements were carried out employing a scanning electron microscope as mentioned before.

2.4. Adsorption experiments

Batch adsorption experiments were performed by adding 0.01 g PAA/CS to a conical flask with 10 mL standard solution, of concentration 100 mg L^{-1} diluted by the stock solution and shaking at 150 rpm, 28 °C. After that, the concentration of supernatant in the system was analyzed by UV-vis spectrophotometer with a wavelength of 650 nm using Arsenazo-III as the complexing agent.

The U(VI) ion removal amounts on PAA/CS hydrogel were calculated as follows:

$$q_e = \frac{C_0 - C_e}{m} V \quad (1)$$

where q_e is the adsorption capacity of the PAA/CS (mg g^{-1}), C_0 is the initial concentration of U(VI) ions before adsorption (mg

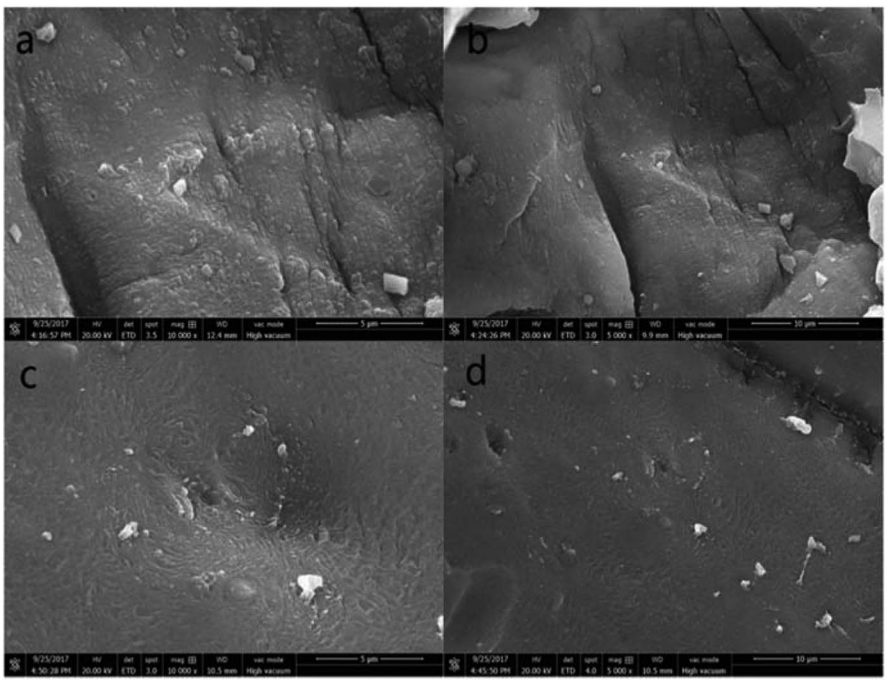

Fig. 2 SEM images of PAA/CS. (a) and (b) Before adsorption, (c) and (d) after adsorption.

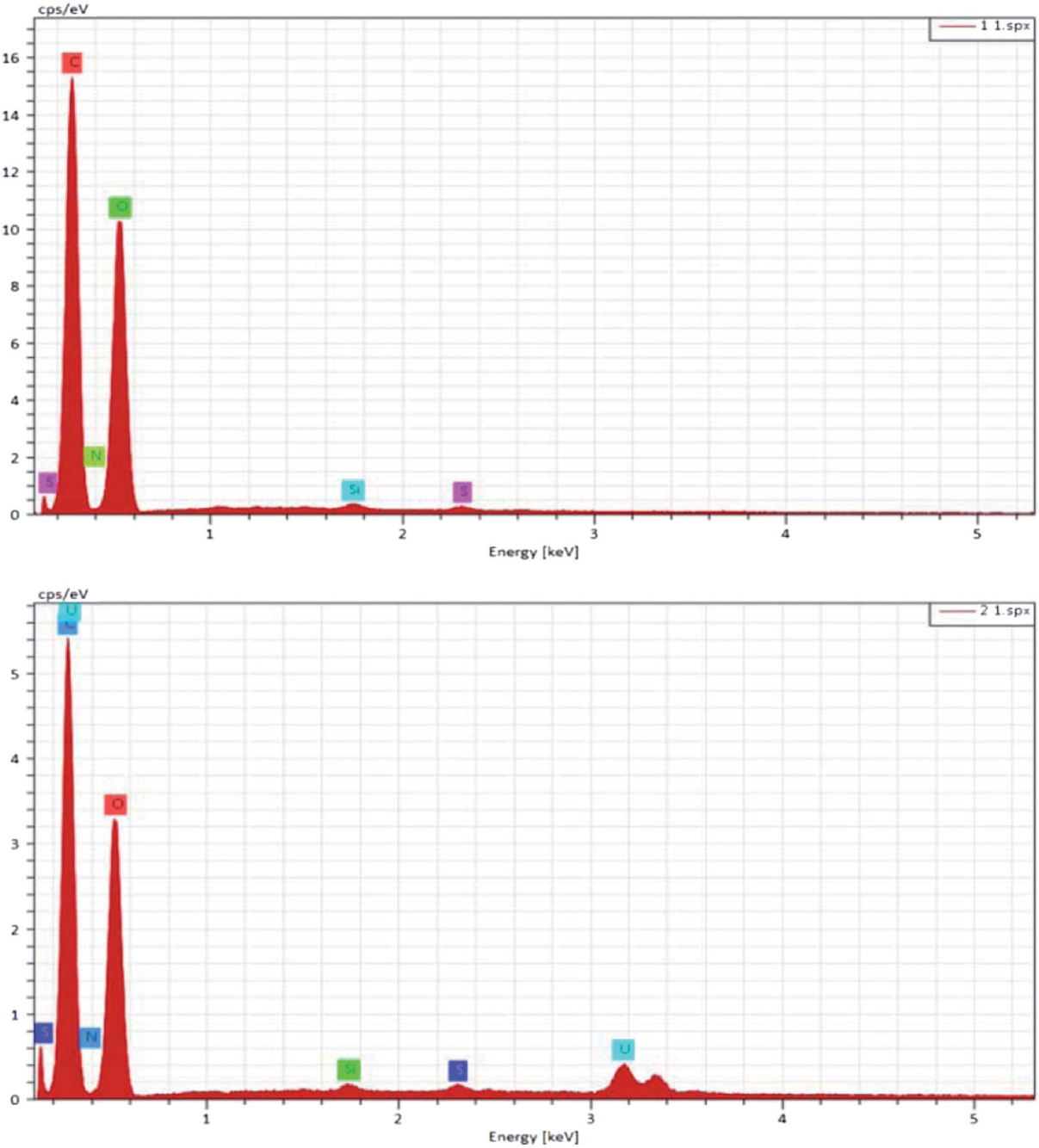

Fig. 3 EDX spectra of PAA/CS. Before adsorption and after adsorption.

L^{-1}), C_e is the final concentration of U(VI) ions after adsorption (mg L^{-1}), V is the volume of U(VI) ion solution (mL), and m is the absorber mass supplied (g).

To investigate the effect of pH on adsorption, the pH value of solution before adsorption was adjusted to 1–5.5 with the diluted HNO_3 (0.1 M) or NaOH (0.1 M) at initial U(VI) ions of 50, 100, and 150 mg L^{-1}.

To assess the effect of initial ion concentrations on adsorption, the PAA/CS of 0.01 g was added to several flasks containing 10 mL solutions in which the initial U(VI) ions concentrations were 20–500 mg L^{-1} and pH 4.0 at 28 °C.

The isotherms were studied by adding 0.01 g PAA/CS in eight equal volume flasks containing 10 mL U(VI) ion solution with initial ion concentrations of 20, 50, 100, 150, 200, 300, 400, and 500 mg L^{-1}, at 28 °C, with shaking for 300 min. The effect of contact time and the adsorption kinetic experiments were conducted using initial uranium concentrations of 50, 100, and 150 mg L^{-1}, at 28 °C, with shaking for 350 min. Finally, the supernatants were taken at different time intervals (10, 20, 35, 50, 80, 110, 170, 230, 290, 350 min) and the residual U(VI) ion concentrations in solution were calculated.

After the adsorption reached equilibrium, the absorbent was soaked in elution solution (0.1 M HNO_3) for about 12 h at room

temperature and washed with distilled water to neutral. The regenerative adsorbent was reused five times.

3. Results and discussion

3.1. Characterization of PAA/CS

The infrared spectra of AA, CS, PAA/CS, and PAA/CS after adsorption in the region of 400–4000 cm^{-1} are depicted in Fig. 1. Strong absorption peaks appeared at 1694 cm^{-1}, which indicated the stretching of the carboxylic group from AA, PAA/CS, and U-PAA/CS complexes. CS shows characteristic peaks at 3251, 1630, 1515, and 1060 cm^{-1} corresponding to the stretching of O–H, amide-I, amide-II, and the stretching of –C–O–C, respectively.[21,22] The peak that disappeared at 1635 cm^{-1} from –C=C– is attributed to polymerization of AA monomer, and the emerging peaks at 1525 cm^{-1} (amide characteristic absorption bands) are assigned to the addition of CS, confirming the PAA/CS product formed. After adsorption, there was a new peak at 928 cm^{-1} from the stretching vibration of O=U=O, suggesting that uranium ions can be absorbed by PAA/CS composite.

Scanning electron microscopy (SEM) images of PAA/CS and U-PAA/CS are shown in Fig. 2. As depicted in Fig. 2(c) and (d), the overall frame structure of composite was not changed after adsorption, which suggested that the gel after adsorption of uranium was no trail of destruction. The surface of the materials became denser and roughened during the diffusion of UO_2^{2+} in many pores of hydrogels. The surface stripe of the adsorbent changed to a spiral, which could be attributed to the swelling of the uranium solution into the interior of the absorbent. The results showed the PAA/CS hydrogels had a strong binding capacity with UO_2^{2+}.

EDX analysis was conducted, and is depicted in Fig. 3. It is worth noting that the absorbent contains three elements, C, O, and N (Table 1), and after adherence of uranium onto the surface of PAA/CS, a new peak of U appeared in the EDX spectrum, confirming that the UO_2^{2+} is successfully captured by PAA/CS.

3.1.1 Effect of initial concentration of the U(IV) ions. The effects of initial U(IV) ions concentrations on the adsorption process by PAA/CS at 28 °C with pH = 4 are presented in Fig. 4, in which it can be seen that adsorption of U(IV) on PAA/CS increased with increasing concentrations of the U(VI) ions. This may be because the increase of concentration decreases mass transfer resistance between the solid and liquid phases.[23] At the same time, with the concentration increased, the particular number of active binding sites determined that adsorption no longer occurred.

3.1.2 Effect of initial pH. The pH of aqueous solution affects the adsorption process as it can influence interaction between different ions in the system, and the adsorption of UO_2^{2+} ions depends on distribution of the uranium species in solution.[24] Fig. 5 shows that the adsorption capacities of PAA/CS enhanced sharply because of deprotonation of the amino groups and carboxyl group with increase of pH from 2 to 4, and then the adsorption capacity showed independent on further increasing of pH and reached a plateau at pH 4, attributed to the fixed amount of $–COO^-$, –OH, and $–NH_2$ on absorber in aqueous solution. The decreased concentration of uranium in the aqueous phase suggests that U(IV) ions are adsorbed through ion-exchange with hydrogen ions on the binding sites formed by amino groups and through electrostatic attraction with carboxyl groups on PAA/CS hydrogel.

3.1.3 Effect of contact time and kinetic studies. Fig. 6(a) shows the trend of adsorption *versus* contact time by PAA/CS. The rate of adsorption at the early stage was faster than that at the latter period, and the maximum adsorption capacity was

Table 1 Elemental composition of the PAA/CS and U-PAA/CS by EDX

Samples	C (%)	N (%)	O (%)	U (%)
PAA/CS	54.66	5.60	39.56	0
U-PAA/CS	51.28	4.36	43.39	0.97

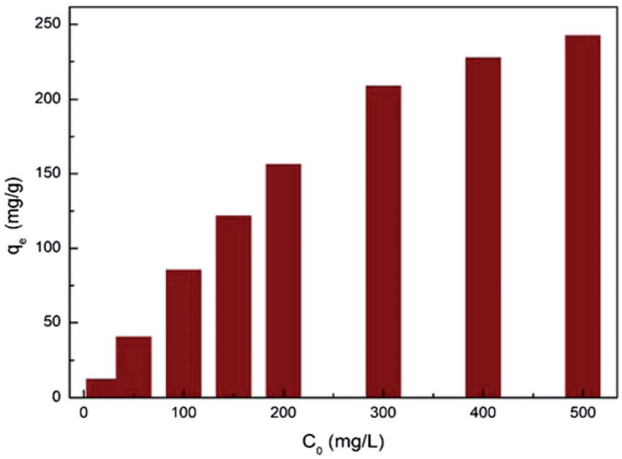

Fig. 4 Effect of initial concentrations (20, 50, 100, 150, 200, 300, 400, 500 mg L^{-1}) on U(VI) removal by PAA/CS hydrogels. (Volume, 10 mL; absorbent dose, 0.01 g; pH value, 4.0; temperature, 28 °C; rotating speed, 150 rpm).

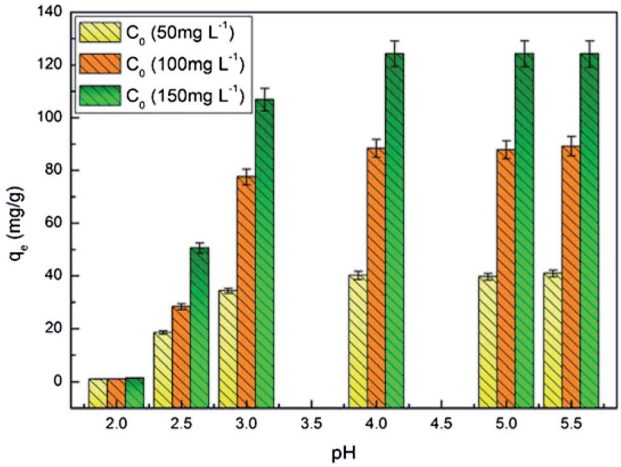

Fig. 5 Effect of contact pH on U(VI) adsorption. (Volume, 10 mL; absorbent dose, 0.01 g; initial concentration, 50, 100, and 150 mg L^{-1}; pH value, 4.0; temperature, 28 °C; rotating speed, 150 rpm).

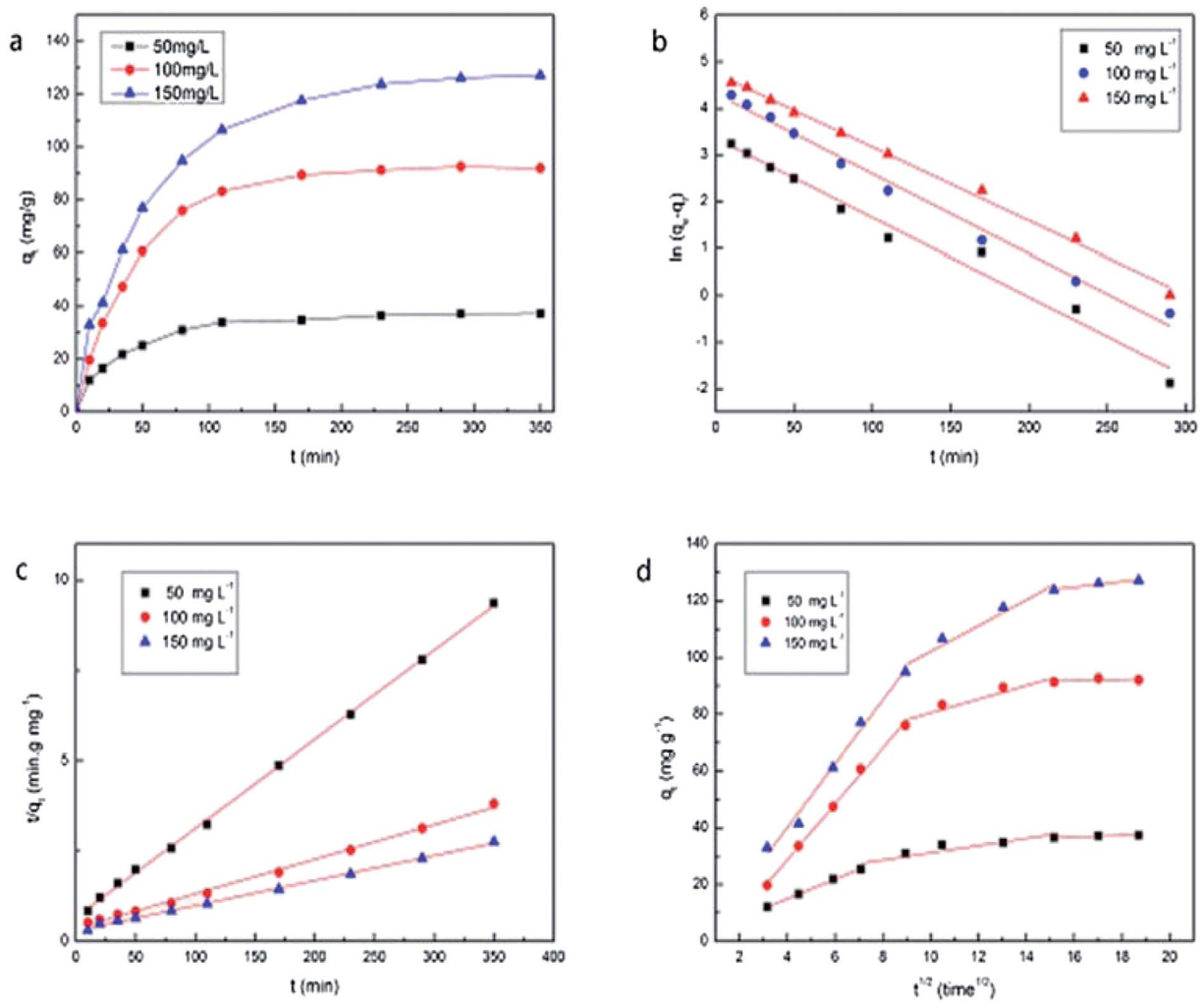

Fig. 6 (a) Effect of contact time on U(VI) adsorption; (b) pseudo-first-order and (c) pseudo-second-order sorption kinetics; (c) intraparticle diffusion kinetics of U(VI) onto PAA/CS at various initial concentrations.

obtained at the equilibrium stage (250 min). To allow most of the binding sites to be occupied by uranium ions and the adsorption end-point to be at a stable stage, 350 min was selected as the reaction time in subsequent experiments.

Kinetic studies revealed the dynamic process and the mechanism of sorption. Pseudo-first-order, pseudo-second-order kinetic models and intra-particle diffusion model are mainly used to fit the experimental data.

The pseudo-first-order model is expressed in the following equation:

$$\ln(q_e - q_t) = \ln q_e - k_1 t \quad (2)$$

The pseudo-second-order model is expressed in the following equation:

$$\frac{t}{q_t} = \frac{1}{k_2 q_e^2} + \frac{t}{q_e} \quad (3)$$

where q_e and q_t represent the absorbed amounts on PAA/CS at equilibrium and time t (min), respectively. k_1 and k_2 (min^{-1}) are the rate constant of the pseudo-first-order model and second-order kinetic equation. t is the contact time of the adsorption process.

In addition, the model of intra-particle diffusion can be expressed as:

$$q_t = k_i t^{1/2} + C \quad (4)$$

where k_i (mg g^{-1} min$^{-1/2}$) is the rate constant of intra-particle diffusion, and C is thickness of the boundary layer.

As shown in Table 2, the k_1, k_2, and q_e values in each formula are calculated from the pseudo-first and the pseudo-second-order models, which showed that the pseudo-second-order model fits the experiment data better as the values of $q_{e,cal}$ are closer to the experimental results ($q_{e,exp}$) and the R^2 of 0.977–0.996 obtained from the pseudo-second-order model were much higher than that calculated from the pseudo-first-order model.

The plots in Fig. 6(d) based on the intra-particle diffusion models provide an explanation of the adsorption process, which emphasizes that adsorption in aqueous solution can be viewed as three steps, instantaneous adsorption or external surface

Table 2 Pseudo-first-order, pseudo-second-order, and intra-particle diffusion kinetic model parameters

	$T = 301$ K, pH = 4		
Kinetic model parameters	50 mg L^{-1}	100 mg L^{-1}	150 mg L^{-1}
Pseudo-first-order model			
$k_1 \times 10^{-2}$	1.896	1.716	1.579
R^2	0.977	0.989	0.996
q_e (mg g^{-1})	28.6619	74.9686	115.8238
Pseudo-second-order model			
$k_2 \times 10^{-4}$	9.285	3.943	1.661
R^2	0.999	0.996	0.998
q_e (mg g^{-1})	40.5186	85.4021	144.0922
$q_{e,exp}$ (mg g^{-1})	37.369	82.731	127.162
Intra-particle diffusion			
k_1	3.4362	9.8428	11.2239
k_2	1.2724	2.4046	4.5495
k_3	0.2118	0.2016	0.9545

adsorption, diffusion into mesopores, and equilibrium stage. The rate of each step follows the order of $k_1 > k_2 > k_3$.

3.1.3 Adsorption isotherm studies. The adsorption isotherm is a model to investigate how the adsorbed ions are distributed over the adsorbent. From the research, Langmuir and Freundlich isotherm models are expressed as in eqn (5) and (6), respectively.

$$q_e = \frac{q_{max} K_L C_e}{1 + K_L C_e} \quad (5)$$

$$q_e = K_F C_e^{1/n} \quad (6)$$

where C_e is the equilibrium concentration of the absorbate (mg L^{-1}), q_e is the amount of absorbed ions at equilibrium (mg g^{-1}). q_{max} represents the maximum adsorption capacity of the absorber (mg g^{-1}). K_L and K_F are the Langmuir adsorption constant and Freundlich constant related to the energy of adsorption (L mg^{-1}). n is the Freundlich constant related to the intensity.

The Temkin isotherm provides an assumption that the free energy of sorption is a function of surface coverage. The interaction of adsorbents and adsorbates has a significant effect on adsorption. The Temkin isotherm is written as:

$$q_e = \frac{RT}{b_T} \ln(a_T C_e) \quad (7)$$

where T is the absolute temperature (K), R is the ideal gas constant (8.314 J mol^{-1} K^{-1}), a_T is the equilibrium binding constant correlating to the maximum binding energy, and b_T is the Temkin isotherm constant.

The Langmuir isotherm model states that adsorption is a simple monolayer adsorption process on a homogeneous surface, while the Freundlich isotherm model predicts the forces between ions cannot be neglected and the surface of the absorbent is not homogeneous.

Fig. 7 shows the fitting plot of the three isotherm models. As can be seen, the Langmuir isotherm model is found to be more in line with the experimental data, with the highest correlation value ($R^2 = 0.964$) revealing a single layer adsorption process. The K_L value from the calculations of the Langmuir isotherm model is 0.02714 and the separation factor constant ($0.0686 < R_L < 0.4243$) suggests that the adsorption between the adsorbent (PAA/CS) and UO_2^{2+} is favorable.

Based on the kinetic and isotherm studies, the mechanism of adsorption is probably a combination of the unpaired electrons of oxygen and nitrogen atoms with uranium ions through coordination bonds.[23]

3.1.4 Recovery experiments and comparison with other adsorbents. The PAA/CS hydrogel was rinsed with 0.1 M HNO_3 solution for investigating the reusable performance of adsorbent. According to Fig. 8, the capacity of composite in absorbing radioactive ions in water only slightly declined (by 4.04%). The outcome shows that the adsorbent in this study could be used at least five times.

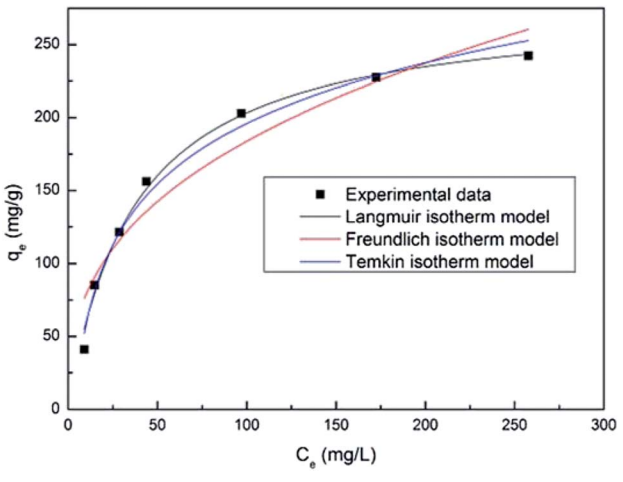

Fig. 7 Langmuir, Freundlich, and Temkin isotherms for adsorption of U(VI) ions onto PAA/CS hydrogels. (Volume, 10 mL; absorbent dose, 0.01 g; initial concentration, 20, 50, 100, 150, 200, 300, 400 and 500 mg L^{-1}; pH value, 4.0; temperature, 28 °C, rotating speed, 150 rpm).

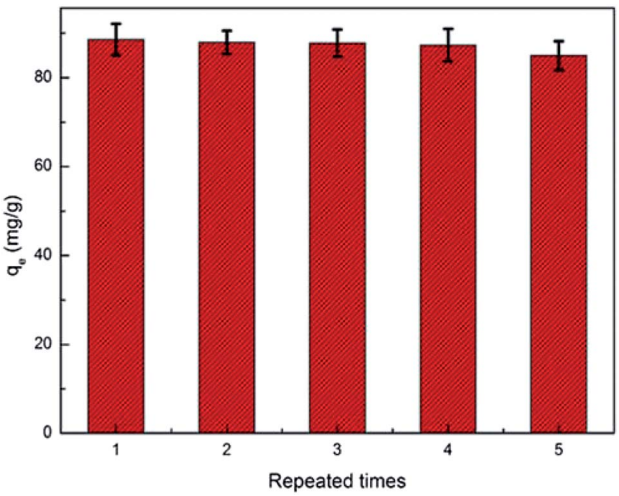

Fig. 8 Adsorption/desorption cycles (initial concentration: 100 mg L^{-1}).

Table 3 Comparison of adsorption capacities for U(VI) ion of various adsorbents

Absorbents	Q_{max} (mg g^{-1})	References
Zeolite	11.13	24
Oxidized activated carbon	25	25
Carboxymethyl cellulose (CMC)-grafted MWCNTs	112	26
Quinoline-8-ol-modified cross-linked chitosan	218	27
RGO	47	28
SA/CMC	101.8	29
AgOH–MWCNTs	140	30
PAA/CS	289.6	This work

As summarized in Table 3, comparison of organic, inorganic materials, and composites applied to extraction of contaminated ions in wastewater conducts that the PAA/CS hydrogel has more advantages including high efficiency of adsorption and simplicity of synthesis process than other adsorption materials.

4. Conclusions

A PAA/CS interpenetrating network hydrogel was prepared successfully in aqueous solution by free radical polymerization, and this hydrogel can be used in a simple and effective method for removal of the uranium from wastewater. The adsorption kinetics of PAA/CS were well described by a pseudo-second-order kinetic model. The experimental data fit the Langmuir model well and the maximum sorption capacity of PAA/CS was 289.6 mg g^{-1}. Analysis of the hydrogel structure after adsorption gave the indication that PAA/CS composites have excellent prospects in management of polluted water.

Conflicts of interest

There are no conflicts to declare.

References

1 D. Yang, S. Song, Y. Zou, X. Wang, S. Yu, T. Wen, H. Wang, T. Hayat, A. Alsaedi and X. Wang, Rational design and synthesis of monodispersed hierarchical SiO_2@layered double hydroxide nanocomposites for efficient removal of pollutants from aqueous solution, *Chem. Eng. J.*, 2017, **323**, 143–152.

2 C. Banerjee, N. Dudwadkar, S. C. Tripathi, P. M. Gandhi, V. Grover, C. P. Kaushik and A. K. Tyagi, Nano-cerium vanadate: A novel inorganic ion exchanger for removal of americium and uranium from simulated aqueous nuclear waste, *J. Hazard. Mater.*, 2014, **280**, 63–70.

3 L. Yuan, M. Sun, X. Liao, L. Y. Zhao, Z. Chai and W. Shi, Solvent extraction of U(VI) by trioctylphosphine oxide using a room-temperature ionic liquid, *Sci. China: Chem.*, 2014, **11**, 1432–1438.

4 Q. Jin, L. Su, G. Montavon, Y. Sun, Z. Chen, Z. Guo and W. Wu, Surface complexation modeling of U(VI) adsorption on granite at ambient/elevated temperature: Experimental and XPS study, *Chem. Geol.*, 2016, **433**, 81–91.

5 H. Zhao, X. Liu, M. Yu, Z. Wang, B. Zhang, H. Ma, M. Wang and J. Li, A Study on the Degree of Amidoximation of Polyacrylonitrile Fibers and Its Effect on Their Capacity to Adsorb Uranyl Ions, *Ind. Eng. Chem. Res.*, 2015, **54**, 3101–3106.

6 H. Liu, R. Wang, H. Jiang, H. Gong and X. Wu, Study on adsorption characteristics of uranyl ions from aqueous solutions using zirconium hydroxide, *J. Radioanal. Nucl. Chem.*, 2015, **308**, 213–220.

7 X. Yang, J. Li, T. Wen, X. Ren, Y. Huang and X. Wang, Adsorption of naphthalene and its derivatives on magnetic graphene composites and the mechanism investigation, *Colloids Surf., A*, 2013, **422**, 118–125.

8 D. Shao, G. Hou, J. Li, T. Wen, X. Ren and X. Wang, PANI/GO as a super adsorbent for the selective adsorption of uranium(VI), *Chem. Eng. J.*, 2014, **255**, 604–612.

9 Y. Wang, Z. Zhang, Y. Liu, X. Cao, Y. Liu and Q. Li, Adsorption of U(VI) from aqueous solution by the carboxyl-mesoporous carbon, *Chem. Eng. J.*, 2012, **198–199**, 246–253.

10 M. A. Dubois, J. F. Dozol, C. Nicotra, J. Serose and C. Massiani, Pyrolysis and incineration of cationic and anionic ion-exchange resins: Identification of volatile degradation compounds, *J. Anal. Appl. Pyrolysis*, 1995, **31**, 129–140.

11 M. Carboni, C. W. Abney, K. M. L. Taylor-Pashow, J. L. Vivero-Escoto and W. Lin, Uranium Sorption with Functionalized Mesoporous Carbon Materials, *Ind. Eng. Chem. Res.*, 2013, **52**, 15187–15197.

12 Z. Li, F. Chen, L. Yuan, Y. Liu, Y. Zhao, Z. Chai and W. Shi, Uranium(VI) adsorption on graphene oxide nanosheets from aqueous solutions, *Chem. Eng. J.*, 2012, **210**, 539–546.

13 S. Simsek and U. Ulusoy, Uranium and lead adsorption onto bentonite and zeolite modified with polyacrylamidoxime, *J. Radioanal. Nucl. Chem.*, 2012, **292**, 41–51.

14 B. Campos, J. Aguilar-Carrillo, M. Algarra, M. A. Gonçalves, E. Rodríguez-Castellón, J. C. G. E. Silva and I. Bobos, Adsorption of uranyl ions on kaolinite, montmorillonite, humic acid and composite clay material, *Appl. Clay Sci.*, 2013, **85**, 53–63.

15 S. Simsek, Adsorption properties of lignin containing bentonite–polyacrylamide composite for UO_2^{2+}ions, *Desalin. Water Treat.*, 2015, **57**, 23790–23799.

16 M. Monier and D. A. Abdel-Latif, Synthesis and characterization of ion-imprinted resin based on carboxymethylcellulose for selective removal of UO_2^{2+}, *Carbohydr. Polym.*, 2013, **97**, 743–752.

17 W. S. Ngah, C. S. Endud and R. Mayanar, Removal of copper(II) ions from aqueous solution onto chitosan and cross-linked chitosan beads, *React. Funct. Polym.*, 2002, **50**, 181–190.

18 Q. Wang, J. L. Mynar, M. Yoshida, E. Lee, M. Lee, K. Okuro, K. Kinbara and T. Aida, High-water-content mouldable

hydrogels by mixing clay and a dendritic molecular binder, *Nature Letters.*, 2010, **463**, 339–343.

19 X. Yi, Z. Xu, Y. Liu, X. Guo, M. Ou and X. Xu, Highly efficient removal of uranium(VI) from wastewater by polyacrylic acid hydrogels, *RSC Adv.*, 2017, **7**, 6278–6287.

20 C. Qiao, X. Ma, J. Zhang and J. Yao, Molecular interactions in gelatin/chitosan composite films, *Food Chem.*, 2017, **235**, 45–50.

21 M. Jridi, S. Hajji, H. B. Ayed, I. Lassoued, A. Mbarek, M. Kammoun, N. Souissi and M. Nasri, Physical, structural, antioxidant and antimicrobial properties of gelatin–chitosancomposite edible films, *Int. J. Biol. Macromol.*, 2014, **67**, 373–379.

22 M. Hosseini, A. Keshtkar and M. Alimoosavian, Electrospun chitosan/baker's yeast nanofibre adsorbent: preparation, characterization and application in heavy metal adsorption, *Bull. Mater. Sci.*, 2015, **4**, 1091–1100.

23 Y. Niu, D. Ying, K. Li, Y. Wang and J. Jia, Fast removal of copper ions from aqueous solution using an ecofriendly fibrous adsorbent, *Chemosphere*, 2016, **161**, 501–509.

24 W. Zou, H. Bai, L. Zhao, K. Li and R. Han, Characterization and properties of zeolite as adsorbent for removal of uranium(VI) from solution in fixed bed column, *J. Radioanal. Nucl. Chem.*, 2011, **288**, 779–788.

25 C. Kütahyalı and M. Eral, Selective adsorption of uranium from aqueous solutions using activated carbon prepared from charcoal by chemical activation, *Sep. Purif. Technol.*, 2004, **40**, 109–114.

26 D. Shao, Z. Jiang, X. Wang, J. Li and Y. Meng, Plasma Induced Grafting Carboxymethyl Cellulose on Multiwalled Carbon Nanotubes for the Removal of UO_2^{2+} from Aqueous Solution, *J. Phys. Chem. B*, 2009, **113**, 860–864.

27 Y. Liu, X. Cao, Z. Le, M. Luo, W. Xu and G. Huang, Pre-Concentration and Determination of Trace Uranium (VI) in Environments using Ion-imprinted Chitosan Resin *via* Solid Phase Extraction, *J. Braz. Chem. Soc.*, 2010, **3**, 533–540.

28 S. Liu, S. Li, H. Zhang, L. Wu, L. Sum and J. Ma, Removal of uranium(VI) from aqueous solution using grapheme oxide and its amine-functionalized composite, *J. Radioanal. Nucl. Chem.*, 2016, **309**, 607–614.

29 L. Wu, X. Lin, X. Zhou and X. Luo, Removal of uranium and fluorine from wastewater by double-functional microsphere adsorbent of SA/CMC loaded with calcium and aluminum, *Appl. Surf. Sci.*, 2016, **384**, 466–479.

30 F. Zare, M. Ghaedi, A. Daneshfar, S. Agarwal, I. Tyagi, T. A. Saleh and V. K. Gupta, Efficient removal of radioactive uranium from solvent phase using AgOH–MWCNTs nanoparticles: Kinetic and thermodynamic study, *Chem. Eng. J.*, 2015, **273**, 296–306.